

Article

DC Flashover Performance of Various Types of Ice-Covered Insulator Strings under Low Air Pressure

Jianlin Hu ^{1,*}, Caixin Sun ^{1,†}, Xingliang Jiang ¹, Daibo Xiao ², Zhijin Zhang ¹ and Lichun Shu ¹

¹ State Key Laboratory of Power Transmission Equipments & System Security and New Technology, College of Electrical Engineering, Chongqing University, Chongqing 400030, China;

E-Mails: xljiang@cqu.edu.cn (X.J.); zhangzhijing@cqu.edu.cn (Z.Z.); leshu@cqu.edu.cn (L.S.)

² Hubei Suizhou Electric Power Supply Company, Suizhou 441300, China;

E-Mail: cqdbxiao@sina.com

† Deceased on 25 November 2011.

* Author to whom correspondence should be addressed; E-Mail: hujianlin@cqu.edu.cn;
Tel.: +86-23-65111172 (ext. 8219); Fax: +86-23-65102442.

Received: 9 April 2012; in revised form: 15 May 2012 / Accepted: 15 May 2012 /

Published: 21 May 2012

Abstract: In this study, icing flashover performance tests of typical DC porcelain, glass, and composite insulators are systematically carried out in a multifunction artificial climate chamber. The DC icing flashover voltages of seven typical insulators under various conditions of icing thickness, pollution severity before icing, string length, and atmospheric pressure are obtained. The relationships between icing thickness, salt deposit density as well as atmospheric pressure and the 50% icing flashover voltage are analyzed, and the formulas are obtained by regression method. In addition, the DC icing flashover voltage correction method of typical porcelain, glass, and composite insulator in the coexisting condition of high altitude, contamination, and icing is proposed.

Keywords: ice-covered insulator string; flashover performance; DC; low air pressure; pollution

1. Introduction

In most cold climate regions of the World, overhead transmission lines and their substations are subject to ice accumulation for an extended period each year due to freezing rain or drizzle, in-cloud icing, icing fog, wet snow, or frost. In addition to mechanical damage due to excessive ice accumulation and dynamic loads caused by wind, the presence of ice and snow on insulators may lead to flashover faults that result in power network outages. In recent years, several incidents related to the flashover of iced insulators have been reported in China, Canada, and other countries [1–11]. In January to February 2008, continuous cryogenic freezing rain and snow disasters occurred in Central China, East China, and South China. A total of 36,740 transmission lines and 2,018 power stations in 13 provinces were damaged by ice accretion. Over 30 million customers in more than 170 countries, approximately half the population of those areas, were also without power for periods of 2 to 15 days. The ice storm resulted in huge financial losses of power systems [11–15].

This problem has motivated research including field observations, laboratory investigation of the icing process, measurement of critical flashover voltage on ice-covered insulators, and fundamental studies of arc development on ice surfaces. Laboratory studies and field experience have shown that the main chronological sequence of events leading to flashover can be roughly summarized as follows: ice accretion along energized insulators is not always uniform because several parts of the insulators are free of ice; these zones are referred to as air gaps. The ice surface melts to form water because of sunshine, a rise in air temperature, condensation, and the heating effect of leakage current. The high conductivity of water film (caused by the rejection of impurities from the solid part toward the liquid portion of drops or droplets during solidification, and by the water pollution) means that voltage drops occur essentially across the air gaps. If the electric field across those gaps is high enough, then corona discharges will be initiated in the form of luminous branched filaments (“streamers”) developing from a common root (the “stem”). Transition to a partial arc is similar to the breakdown process in air; that is, when the physical conditions required for the stem to evolve into an arc channel are reached. This transition can lead to the development of local arcs across the air gaps, causing a substantial increase in leakage current and a concomitant melting of ice. Under sufficient electrical stress, arcs propagate along the ice surface, forming a white arc. When the white arc reaches critical length, the whole insulator suddenly undergoes a complete flashover [2,4,9–11,16–20].

Flashover on an ice surface is an extremely complex phenomenon resulting from the interaction of the following factors: electric field, wet and polluted ice surface, presence of air gaps at the ice surface, environmental conditions, and the complex geometric shape of ice-covered insulators. In Canada, Farzaneh *et al.* have carried out a host of investigations on ice-covered post insulators and suspension insulator strings in a climate chamber. They obtained the concerned flashover performance and the rules influencing how icing conditions, degree of ice accretion, electrical conductivity of freezing water, and insulator length affect flashover voltage, and established a prediction model for icing flashover voltage [9–11,16–20]. Due to limited experimental conditions, these studies mainly focused on post insulators and suspension insulator strings shorter than 1 m, with a few focused on DC flashover performance of long-string ice-covered insulators. In China, utilities such as China Electric Power Research Institute and Chongqing University have carried out numerous studies on the flashover performance of short-string ice-covered insulators since the 1980s. The experimental results

indicated that the characteristic exponent expressing the effects of atmospheric pressure on icing flashover voltage falls in the range of 0.40 to 0.64, and the characteristic exponent expressing the effects of ice accumulation is in the range of 0.088 to 0.143 [4,5,9–11,21–33]. Thus, the design of an external insulation for ultra-high DC transmission lines under combined conditions of high altitude, contamination, and icing remains a technical puzzle. In short, systematic studies on the DC flashover performance of long-string ice-covered insulators under combined conditions of high altitude, pollution, and icing are lacking.

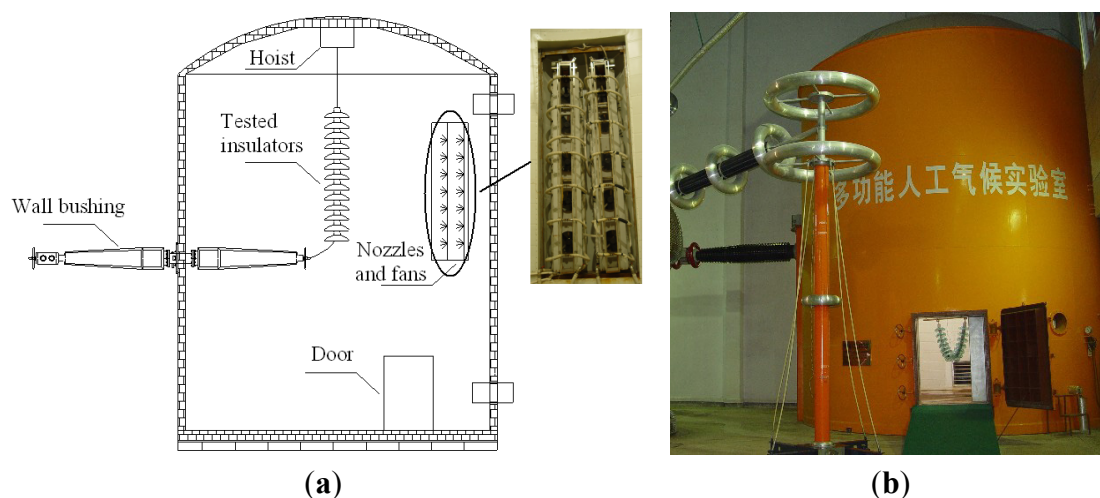
Many Ultra-high Voltage (UHV) DC transmission lines are being constructed and operated in China, most of which need to cross regions of high altitude, pollution, and icing. However, the external insulation discharge characteristic under coexisting conditions of high altitude, pollution, and icing, which is crucial to UHV power transmission construction and power grid development, is an unsolved problem. The present paper systematically explores the DC flashover performance of typical long porcelain, glass strings, and composite insulators under the coexisting conditions of high altitude, pollution, and icing in the multifunction artificial climate chamber of Chongqing University. Additionally, it analyzes the effect of ice thickness, pollution severity, and altitude on flashover voltages of ice-covered insulator strings.

2. Test Facilities and Procedures

2.1. Test Facilities

The experimental investigations were carried out in the multifunction artificial climate chamber in the High Voltage and Insulation Technological Laboratory of Chongqing University. The artificial climate chamber has a diameter of 7.8 m and a height of 11.6 m (Figure 1). It mainly consists of a refrigeration system, a vacuum-pumping system, a spraying system, and a wind velocity regulating system.

Figure 1. The artificial climate chamber in Chongqing University. (a) Schematic of the artificial climate chamber; (b) Photograph of the artificial climate chamber.

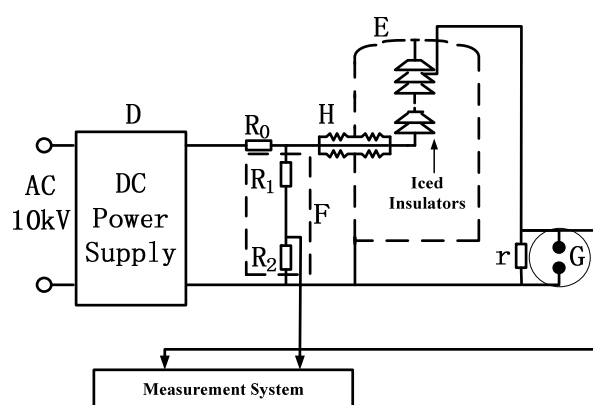


Air temperature in the artificial climate chamber is controlled by a proportional integral and differential system with a precision of about ± 0.5 °C. Minimum temperature in the chamber can be

adjusted to $-45\text{ }^{\circ}\text{C} \pm 1\text{ }^{\circ}\text{C}$. Air pressure in the chamber can be as low as 30 kPa, capable of simulating the atmospheric conditions at an altitude of 7000 m. The spraying system consists of two rows of fog nozzles customized according to standards [34,35] and mounted on an oscillating support parallel to the axis of the insulators at a distance of 3.5 m [Figure 1(a)]. The spraying system is 3.36 m high and 0.43 m wide. The oscillating movement helps keep the mean liquid water content approximately constant along the vertical axis of the insulators, thus forming ice with a uniform thickness along the insulator string. A relatively uniform wind is obtained using a system of 10 fans placed in a tapering box with a diffusing honeycomb panel. Wind velocity in the chamber can be adjusted to 0 m/s to 12 m/s.

Figure 2 shows the schematic diagram of the ice-covered insulator flashover. In the circuit, D is DC test power supply, which is a $\pm 600\text{-kV}/0.5\text{-A}$ cascade rectifying circuit controlled by the thyristor voltage–current feedback system. The technical parameters of DC test power supply are as follows: power supply = AC 10kV, maximum output voltage = 600 kV, ripple factor of the test voltage for a 500 mA current with a resistive load $<3\%$, relative voltage drop occurring during individual tests resulting in withstand $\leq 5\%$, and relative voltage overshoot due to load-release caused by the extinction of electrical discharges on insulator surface $\leq 8\%$. F is the ZGF-600 resistive potential divider. R_1 and R_2 are the resistors. The potential divider is connected to the high voltage, and a definite fraction of the total voltage is measured by a low-voltage voltmeter. Measurement accuracy of the potential divider is 0.5%. R_0 is a current-limiting resistor. H is a tailor-made 330 kV class wall bushing through which the power supply is introduced to the test sample. The dry arcing distance of the wall bushing is 2.73 m, and the unified specific creepage distance is 25 mm/kV. The 30-min power frequency withstand voltage of the wall bushing is 650 kVrms. E represents the multifunction artificial climate chamber, r is a current shunt, and G is the protective discharge tube.

Figure 2. Schematic diagram of the DC test circuit.



2.2. Specimens

The specimens are typical DC porcelain insulators (XZP-210 and XZP-300), typical DC glass insulators (LXZP-210 and LXZP-300), and dc SIR composite long-rod insulators (Type A, Type B, and Type C). The parameters and profiles of the specimens are shown in Tables 1 and 2 and Figures 3 and 4, respectively.

Table 1. Parameters of porcelain and glass insulators.

Type	Profile parameters (mm)			Configuration
	Shed Diameter	Unit Spacing	Leakage Distance	
XZP-210	320	170	545	Figure 3a
XZP-300	400	195	635	Figure 3b
LXZP-210	320	170	545	Figure 3c
LXZP-300	400	195	635	Figure 3d

Table 2. Dimensions of the test composite insulators.

Type	Profile parameters (mm)				Configuration
	Shed Diameter	Dry Arc Distance	Leakage Distance	Housing Diameter	
A	175(big shed) 87.5(small shed)	2195	7393	39	Figure 4a
B	164(big shed) 125(small shed)	2290	7588	32	Figure 4b
C	190(big shed) 110(small shed)	3600	13100	45	Figure 4c

Figure 3. Profiles of test porcelain and glass insulators.

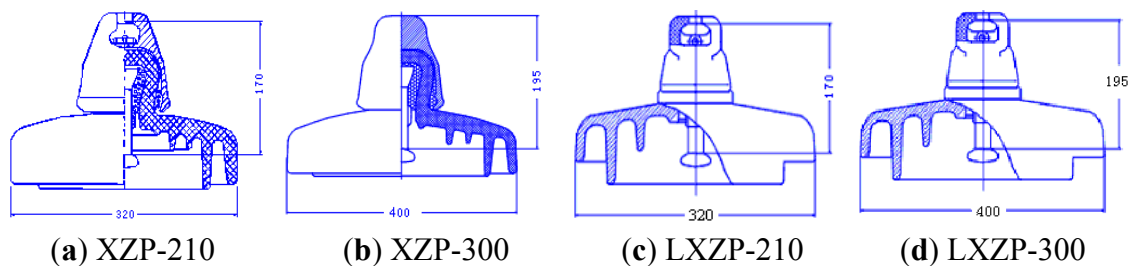
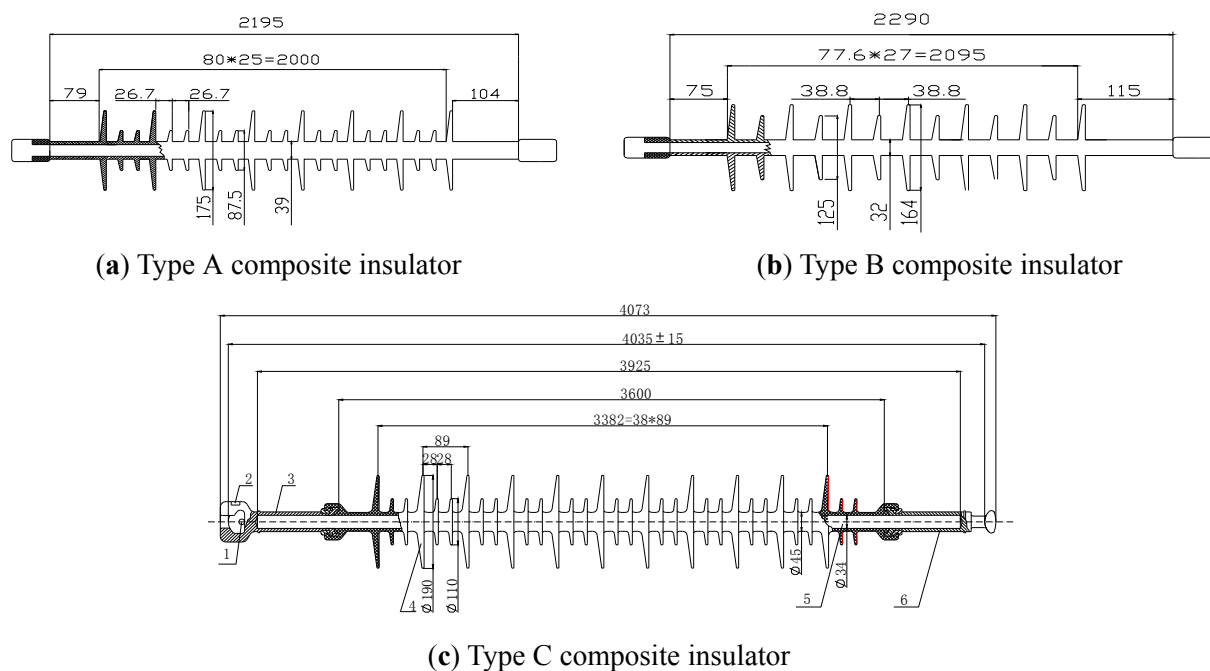


Figure 4. Profiles of test composite insulators.



2.3. Test Procedures and Methods

(1) Preparation: Before the tests, all samples were carefully cleaned to remove all traces of dirt and grease, and then dried naturally.

(2) Artificial polluting: Insulators might be polluted before or during icing. The latter is due to the high water conductivity of the super-cooled water. Accident surveys show that most flashovers of insulator strings of in China's transmission lines result from the pollution on insulators before icing. Rain conductivity is not very high in most mountainous regions in China, and icing often occurs in those areas with freezing water conductivity of 80 $\mu\text{S}/\text{cm}$ to 120 $\mu\text{S}/\text{cm}$. Thus, in this paper, the solid layer method was used to form the pollution layer on the samples before ice deposit.

According to IEC 60507 [34], the surfaces of specimens are contaminated with a suspension of sodium chloride and kieselguhr, which simulates the electric and inert materials, respectively. In this investigation, the salt deposit densities (SDD) were 0.03, 0.05, 0.08, and 0.15 mg/cm^2 , respectively, and the ratio of SDD to nonsoluble deposit density (NSDD) was 1:6. The contamination layer on specimens dried naturally for 24 h.

(3) Ice deposit: The specimens were suspended vertically from the hoist at the center of the chamber and rotated at 1 rpm. When the temperature in the chamber decreased to $-7\text{ }^\circ\text{C}$, the surface of the insulators was wetted by the sprayer and covered with a 1 mm to 2 mm ice layer to ensure the pollution layer was not cleared away. The spraying system was then used to form wet-grown ice on insulators without service voltage. Glaze with icicles is known as the most dangerous type of ice associated with a high probability of flashover on insulators [9]. To ensure the formation of wet-grown ice on the test insulators, the experimental parameters shown in Table 3 are introduced in this study. In such case, the density of wet-grown ice formed on the composite insulators was about 0.84 g/cm^3 to 0.89 g/cm^3 .

Table 3. Experimental ice deposit parameters.

Droplet (μm)	Freezing water conductivity ($\mu\text{S}/\text{cm}$)	Freezing water flux ($\text{L}/\text{h}\cdot\text{m}^2$)	Air temperature ($^\circ\text{C}$)	Wind velocity (m/s)
80	100	90 *	$-7\sim-5$	3.5 *

* except when precise.

The amount of ice accumulated on insulators can influence their flashover voltages considerably. The severity of ice accumulation on insulators is considered according to different factors such as the weight and thickness of ice on the insulators themselves, or by measuring the thickness of the ice on a monitoring cylinder [3,4,9–11]. In the present investigation, the average ice thickness is measured in the applied water exposure zone on a monitoring rotating cylinder, with a diameter of 28 mm and rotating at 1 rpm, installed near the test insulator. The longitudinal axis at each end of the test specimen is horizontally placed to receive the same general wetting as the insulator under test.

(4) Flashover test for ice-covered insulators: Field observation and laboratory investigations show that the flashover of an ice-covered insulators usually occurs during ice melting due to the rise of ambient temperature [11,26]. Therefore, an objective of this paper is to explore the relation between various factors inclusive of ice thickness, altitude, pollution severity, and DC 50% flashover

voltages $U_{50\%}$ of ice-covered insulators in the ice-melting period. The flashover test method is summarized below:

- (i) Stop spraying steam fog when ice thickness reaches the target value and then remove the monitoring cylinder;
- (ii) Lift the iced insulator by the hoist above the wall bushing, and connect the conductor between the wall bushing and the bottom of insulator;
- (iii) Maintain the air temperature at $-7\text{ }^{\circ}\text{C}$ for 15 min to guarantee complete hardening of the ice and equalization of both insulator and ice temperatures;
- (iv) Open the door of the climate chamber to raise the temperature rapidly to $-2\text{ }^{\circ}\text{C}$, and then close the door to recover the temperature to $-1.0\text{ }^{\circ}\text{C}$ to $0.5\text{ }^{\circ}\text{C}$ at a speed of $2\text{ }^{\circ}\text{C/h}$ to $3\text{ }^{\circ}\text{C/h}$;
- (v) Apply the flashover voltage to the iced insulator when the ice surface is lucidus and with a layer of water film. First, increase the voltage at a high rate (about 15 kV/s) to the value of about 75% of predicted flashover voltage U_p , and then change the rate to the value of $2\% \times U_p/\text{s}$ until the flashover. Finally, record the flashover voltage U_f ;
- (vi) Repeat the procedure after 2 to 3 min. Stop the flashover test when most of the ice on the insulator is melted. The minimum flashover voltage $U_{f\min}$ of the test specimen can then be gained;
- (vii) Apply the test procedure (i–vi) to another specimen with a similar ice accretion.

Repeat the test procedure (i–vi) for at least 10 specimens under similar icing conditions. The minimum flashover voltage $U_{f\min}$ for every test specimen can be gained. The 50% flashover voltage $U_{50\%}$ and standard deviation σ can thus be calculated as follows:

$$\begin{cases} U_{50\%} = (\sum_{i=1}^N U_{f\min}(i)) / N \\ \sigma = \sqrt{(\sum_{i=1}^N (U_{f\min}(i) - U_{50\%})^2) / N} \end{cases} \quad (1)$$

where $U_{f\min}(i)$ is the value of minimum flashover voltage of the i th test specimen, kV. N is the valid test specimens in actual experiments, $N \geq 10$.

2.4. Simulation of High Altitude

Low atmospheric pressure in the chamber is used to simulate high-altitude conditions. Atmospheric pressure P (in kPa) is the synthetical reflection of the atmospheric temperature t (in $^{\circ}\text{C}$), the relative density δ_d of dry air, and the absolute humidity h_a (in g/cm^3) of air [31,34]. Thus, P can be used to characterize the influence of atmospheric parameters on the discharge voltage. References [31,34] show that the relationship between atmospheric pressure and altitude H (in km) can be expressed as follows:

$$H = 45.1 \times \left(1 - (P / P_0)^{0.1866}\right) \quad (2)$$

where P_0 is the standard atmospheric pressure (101.3 kPa). In this paper, the altitudes of 232, 1000, 2000, and 3000 m were simulated in the chamber with atmospheric pressures of 98.6, 89.8, 79.5, and 70.1 kPa, respectively.

3. Results and Analysis

3.1. DC Flashover Characteristics of Iced Insulators under Low Atmospheric Pressure

The study includes numerous experiments on DC flashover characteristics of typical DC porcelain insulators (XZP-210, XZP-300), glass insulators (LXZP-210, LXZP-300), and composite insulators in the artificial climate chamber, where a high-altitude low atmospheric pressure is imitated based on the aforementioned artificial icing test methods. The study also explores the effects of various factors including ice thickness, pollution severity on insulator surfaces before ice accretion, and atmospheric pressure on the flashover performance of various types of insulators.

3.1.1. Relationship between $U_{50\%}$ and Ice Thickness d

Degree of insulator ice accretion is one of the most important factors affecting flashover voltage, with ice weight, ice thickness, *etc.* as the representative parameters. Uneven icing on insulators makes it difficult to measure ice weight and ice thickness on them. Furthermore, under the same icing conditions, ice weight and ice thickness on insulators are greatly affected by the insulator type, shed diameter, and installment placement. Farzaneh [4] found that for insulators of different types and shed diameters, their ice weights are almost in a linear relationship with the thickness of ice accumulated on a monitoring rotating cylinder under the same icing environment. In addition, the thickness of ice on the monitoring rotating cylinder can directly represent the ice accretion degree because of its convenient measurement. The study uses ice thickness d of ice accumulated on a monitoring rotating cylinder as the characteristic to explore the effects of ice accretion degree of insulators on the flashover voltage.

The current study carries out research on the relationship between $U_{50\%}$ and ice thickness d of the monitoring rotating cylinder with DC insulator strings XZP-210 and XZP-300 and two types of ± 500 kV DC composite insulators Type A and Type B at altitudes of 232 and 3000 m, and with SDD of 0.05 and 0.15 mg/cm², respectively. In the test, porcelain insulator strings comprise 15 pieces. The results are shown in Figures 5–7, with a standard deviation of 2.7% to 7.2%.

Figure 5. The relationship of $U_{50\%}$ and d of XZP-210 insulator string covered with ice ($N = 15$).

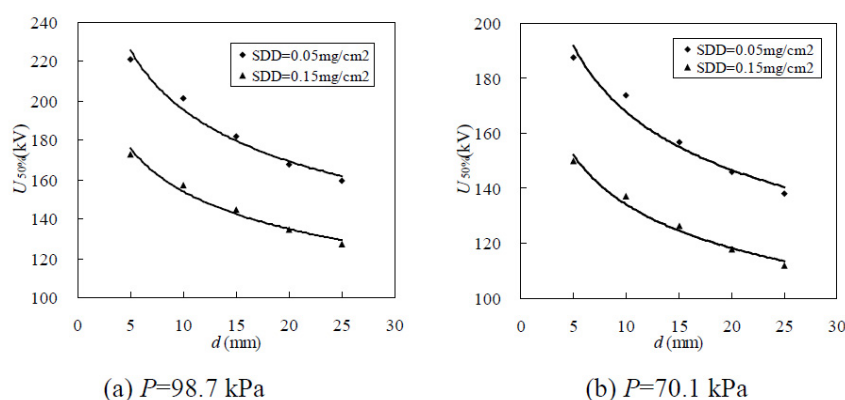


Figure 6. The relationship of $U_{50\%}$ and d of XZP-300 insulator strings covered with ice ($N = 15$).

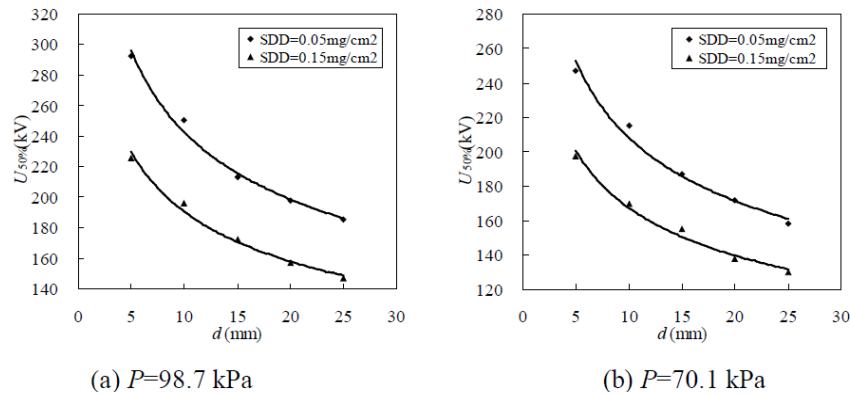
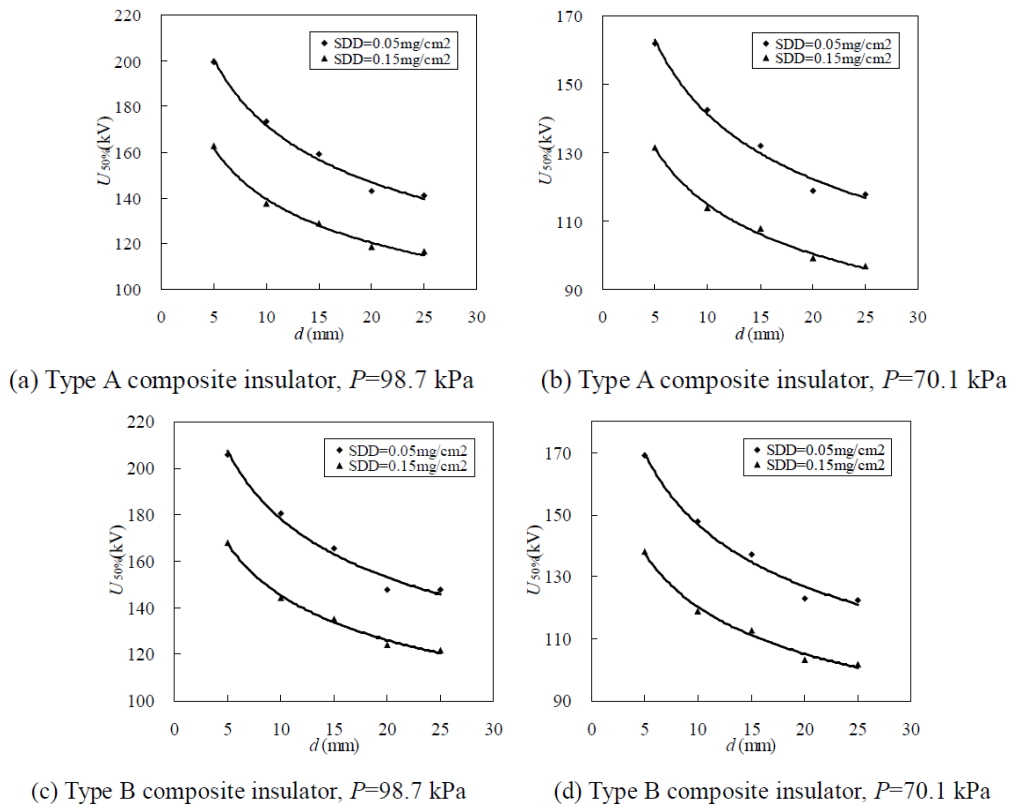


Figure 7. Relationship of $U_{50\%}$ and d of composite insulators covered with ice ($N = 15$).



Experimental results to date [4,11,31] show that the relationship between $U_{50\%}$ and ice thickness can be expressed as:

$$U_{50\%} = A_d \times d^{-c} \tag{3}$$

where A_d is a constant whose value is related to the pollution severity before icing, insulator profile, and material, *etc.*; d is the ice thickness on the monitoring cylinder in mm; and c is the characteristic exponent characterizing the influence of ice thickness on icing flashover voltage $U_{50\%}$. The bigger the value of c , the more obvious the effects of ice thickness on flashover voltage.

The values of A_d and c are obtained by applying regression to the results in Figures 5–7 based on Equation (3). The fitting values and the correlation coefficient R^2 of the regression curve are shown in Table 4.

Table 4. Fitting values of A_d , c , and R^2 according to the test results in Figures 5 to Figure 7 with Equation (3).

Type	SDD (mg/cm^2)	$H = 232 \text{ m}/P = 98.7 \text{ kPa}$			$H = 3000 \text{ m}/P = 70.1 \text{ kPa}$		
		A_d	c	R^2	A_d	c	R^2
XZP-210 (15-unit string)	0.05	315.3	0.208	0.976	261.9	0.194	0.964
	0.15	239.2	0.191	0.978	203.6	0.182	0.979
XZP-300 (15-unit string)	0.05	470.6	0.288	0.978	428.2	0.279	0.984
	0.15	354.5	0.270	0.987	360.5	0.261	0.985
Type A composite insulator	0.05	288.8	0.226	0.985	227.4	0.207	0.982
	0.15	227.6	0.213	0.990	179.1	0.193	0.991
Type B composite insulator	0.05	295.2	0.217	0.978	238.0	0.210	0.980
	0.15	232.8	0.205	0.991	187.7	0.193	0.991
	0.15	238.5	0.211	0.980	186.2	0.190	0.966

Based on Figures 5–7 and Table 4, the following conclusions can be reached:

(i) With the increase of thickness d of ice on the monitoring cylinder, all the $U_{50\%}$ of the two types of porcelain insulator strings and two DC composite insulators of different sheds decrease, which have a negative power-function relationship with ice thickness d . For the four types of insulator strings tested, the value of characteristic exponent c is between 0.182 and 0.288 under different conditions of pollution and altitude.

(ii) Characteristic exponent c is related to insulator type. Take $P = 98.7 \text{ kPa}$, $SDD = 0.05 \text{ mg}/\text{cm}^2$ as an example. The value of c is 0.208, 0.288, 0.226, and 0.217, respectively, for XZP-210, XZP-300 DC porcelain insulator strings and Type A and Type B $\pm 500 \text{ kV}$ DC composite insulators. The value of c for XZP-300 insulator strings is bigger than that for XZP-210 insulator strings, which means that compared with XZP-210 insulator strings, $U_{50\%}$ of XZP-300 insulator strings is more affected by ice thickness. As for XZP-300 insulator strings with bigger unit spacing, when the ice thickness is relatively small, the longer air gap of XZP-300 insulator strings brings higher flashover voltage in comparison with that of XZP-210 insulators. With the increase of ice thickness, icicles on the edge of the insulator shed gradually grow and the effects of the insulators' shed profile on the flashover voltage decrease when the insulators' sheds are bridged completely by icicles. For example, with $d = 25 \text{ mm}$ and under the same pollution severity and air pressure conditions, the flashover voltage per unit length of XZP-300 insulator strings approximates that of XZP-210 insulator strings. This finding is also true for the two types of composite insulators of different sheds. Type A composite insulator consists of one big shed and two small sheds, with the shed diameter gap of 87.5 mm. Type B composite insulator is of the common big shed and small shed structure, with the shed diameter gap of 77.6 mm. Compared with Type B composite insulators, Type A composite insulators have greater shed distance between two big sheds and the sheds of Type A composite cannot be easily bridged by icicles in light icing conditions, resulting in a higher $U_{50\%}$ flashover voltage. The shed profile no longer affects the flashover voltage when the ice thickness of the monitoring cylinder reaches a certain degree and the sheds of composite insulators tested are bridged completely by icicles. As a result, the flashover voltages per unit dry arc length of Type A and Type B composite insulators are close to each other. The

flashover voltage of Type A insulators is more likely to be affected by ice thickness, with a bigger c value in comparison with Type B insulators.

(iii) Characteristic exponent c is related to the pollution severity before icing SDD . For all the four types of insulators, the value of c decreases with the increase of SDD at different altitudes. That is, the more serious the pollution, the smaller the effects of ice thickness on $U_{50\%}$. For example, with $P = 98.7$ kPa, $SDD = 0.05, 0.15$ mg/cm², the value of c for XZP-210 insulator is 0.028 and 0.191, respectively.

(iv) Characteristic exponent is related to the altitude. With the increase of altitude, the value of c gradually decreases, that is, ice thickness affects $U_{50\%}$ less at high altitude than at low altitude. For example, under the condition of $P = 98.7$ kPa, $SDD = 0.05$ mg/cm² when d increases from 5 mm to 20 mm, $U_{50\%}$ for XZP-210 insulator strings lowers by 24.1% and with $P = 70.1$ kPa, it lowers by 16.4%. The possible reasons are as follows: there is a bigger probability for the flashover of ice-covered insulator strings to happen along the ice surface or there may be arc floating for DC flashover of ice-covered insulators. If the probability that the latter phenomenon will happen becomes bigger, the effect of ice thickness on the arc decreases.

(v) The constant A_d is related to insulator types, pollution severity of ice-covered insulator, and altitude. For different types of insulator strings, the constant A_d , in general, increases with pollution degree and decreases with the increase of altitude.

3.1.2. The Effects of SDD on $U_{50\%}$

(1) Porcelain and glass insulator strings. The study investigates DC flashover voltage $U_{50\%}$ of four types of DC insulator strings with a string length of 15 pieces under the altitude conditions of 232, 1000, 2000, and 3000 m, respectively; SDD of 0.03, 0.05, 0.08, and 0.15 mg/cm², respectively; and d of 10 and 20 mm, respectively in the artificial climate chamber. The results, with the standard deviation of 3.1% to 6.9%, are shown in Figure 7.

Icing on insulators is regarded as a special type of pollution. Pollution flashover voltage of DC insulators decreases with the growing pollution severity. The relationship between $U_{50\%}$ and SDD can be expressed as follows [22,31]:

$$U_{50\%} = A_S \times (SDD)^{-b} \quad (4)$$

where A_S is a coefficient related to insulator types, material, voltage polarity, etc.; SDD is the salt deposit before icing, in mg/cm²; b is the characteristic exponent showing the effects of SDD on $U_{50\%}$ related to many factors such as insulator type, air pressure, and voltage polarity.

As is seen in Figure 8, $U_{50\%}$ of four types of porcelain and glass DC insulator strings decreases with the increase of SDD , following the similar relationship expressed in Equation (4). Applying regression to the results in Figure 8 according to Equation (4), the values of A_S , b , and correlation coefficient R^2 of the four types of DC insulator strings under the conditions of different ice thickness and atmospheric pressures can be obtained.

Figure 8. Relationship between $U_{50\%}$ and SDD of insulator strings covered with ice.

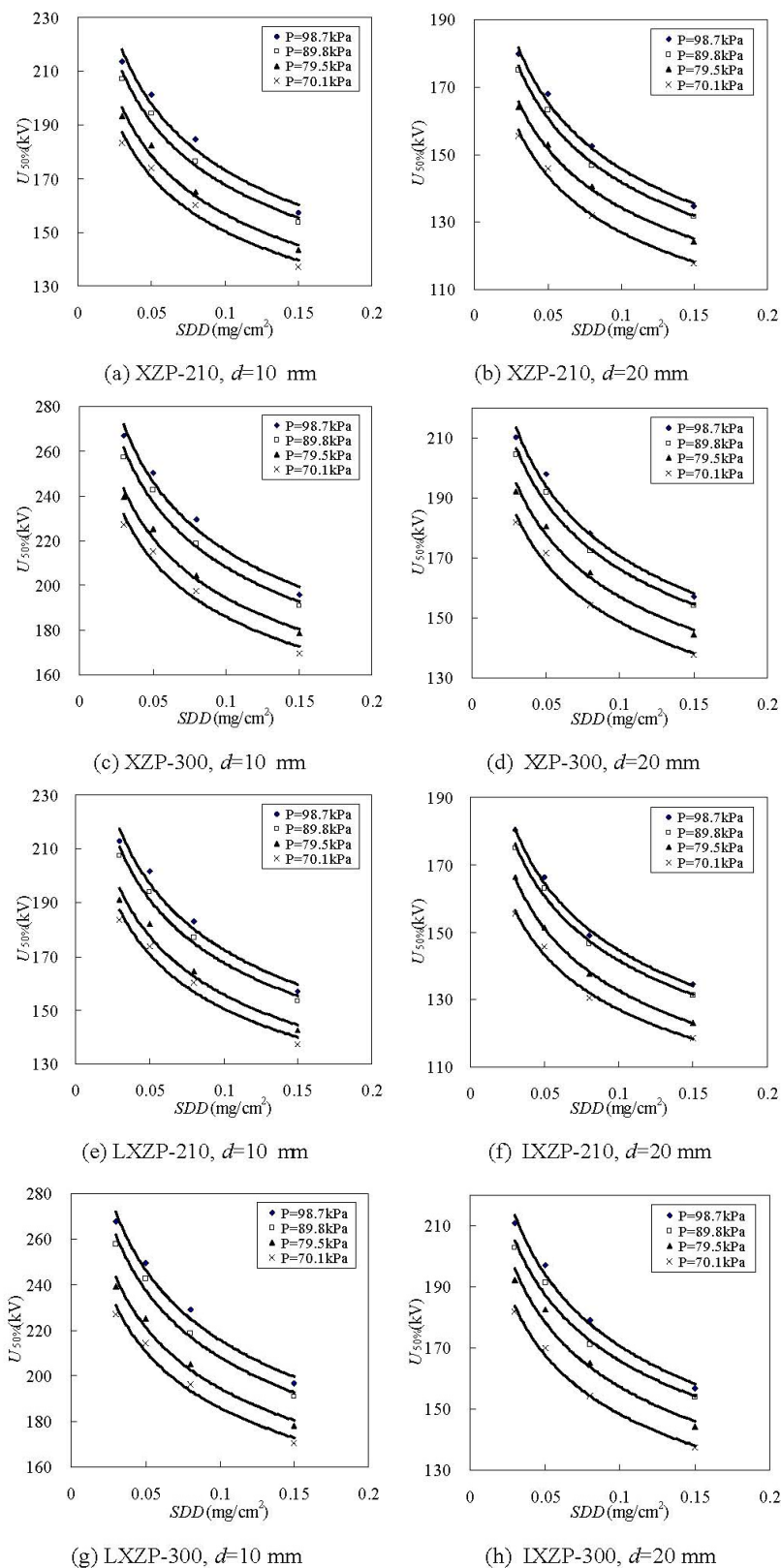


Table 5. Fitting values of A_s , b , and R^2 according to the test results in Figure 8 with Equation (4).

Type	Ice thickness d (mm)	Fitting values	H (m)/ P (kPa)			
			232/98.6	1000/89.8	2000/79.5	3000/70.1
XZP-210	10	A_s	111.5	108.9	101.7	98.8
		b	0.191	0.189	0.188	0.183
		R^2	0.971	0.985	0.981	0.965
	20	A_s	95.7	93.5	89.7	84.4
		b	0.183	0.181	0.175	0.177
		R^2	0.992	0.992	0.993	0.991
XZP-300	10	A_s	138.2	134.5	126.8	121.9
		b	0.193	0.190	0.186	0.183
		R^2	0.976	0.982	0.984	0.970
	20	A_s	111.3	109.7	104.0	98.6
		b	0.186	0.181	0.179	0.179
		R^2	0.986	0.988	0.985	0.986
LXZP-210	10	A_s	110.8	108.6	101.3	99.2
		b	0.192	0.190	0.187	0.181
		R^2	0.971	0.986	0.972	0.970
	20	A_s	94.4	93.1	86.3	85.3
		b	0.185	0.182	0.187	0.173
		R^2	0.994	0.992	0.999	0.989
LXZP-300	10	A_s	138.7	134.2	126.9	122.8
		b	0.192	0.191	0.186	0.180
		R^2	0.983	0.983	0.982	0.978
	20	A_s	111.2	110.2	103.3	98.6
		b	0.186	0.177	0.182	0.177
		R^2	0.989	0.976	0.976	0.994

The following conclusions can be obtained from Figure 8 and Table 5:

(i) The characteristic exponent b indicating the influence of pollution severity SDD before icing on $U_{50\%}$ of porcelain and glass insulator strings is 0.177 to 0.193, and is related to insulator type, altitude or atmospheric pressure, and ice thickness, among other factors.

(ii) b is related to altitude or atmospheric pressure. With the increase of altitude or the decrease of atmospheric pressure, d follows a downward trend, which means that the lower the atmospheric pressure, the smaller the effects of SDD on $U_{50\%}$. For example, with $d = 10$ mm, when P is 98.7, 89.8, 79.5, and 70.1 kPa, b is 0.191, 0.189, 0.188, and 0.183 accordingly. That is, the lower the atmospheric pressure, the lesser the influence of pollution severity on the DC flashover performance of ice-covered insulators. The reason is that during the flashover process of DC icing, partial arcs show floating phenomenon, and with the increasing altitude, the arc floating phenomenon becomes more serious, which makes the development of arcs less affected by pollution.

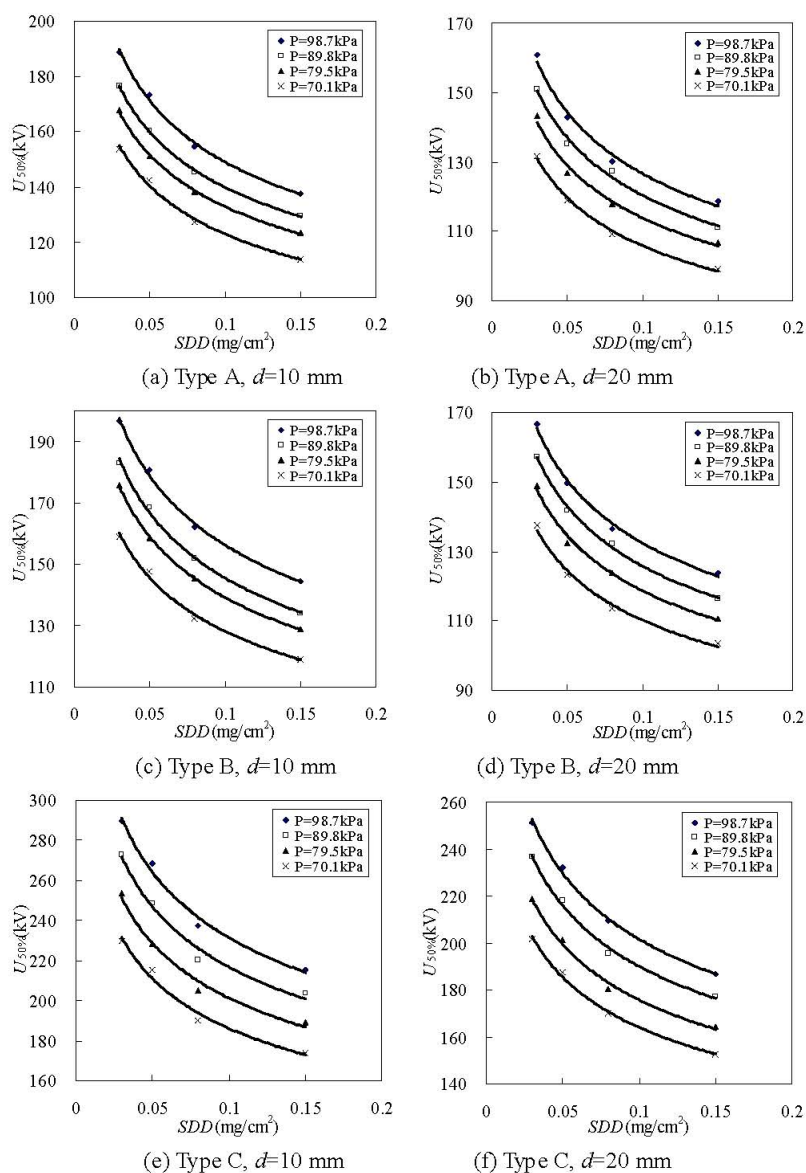
(iii) b is related to ice thickness. The general trend is that exponent b becomes smaller with the growing ice thickness, that is, with the increase of ice thickness, the icing flashover voltage is less

affected by pollution. For example, for the XZP-210 insulator string, with $P = 89.8$ kPa and $d = 10$ mm, b is 0.189; with $d = 20$ mm, b is 0.181.

(iv) b is related to the insulator structure, whose effects on b is generally smaller than those of atmospheric pressure and ice thickness for the four types of porcelain and glass insulators used in the present study. For example, with $P = 98.9$ kPa, $d = 10$ mm, the values of b are 0.191 for porcelain DC insulator XZP-210 and 0.193 for porcelain DC insulator XZP-300. Under other conditions, the maximum difference value is only 0.003.

(2) Composite insulators. The study explores $U_{50\%}$ of Type A and Type B ± 500 kV DC composite insulators of two shed structures and Type C ± 800 kV UHV DC composite insulator at altitudes of 232, 1000, 2000, and 3000 m, respectively, with SDD of 0.03, 0.05, 0.08, and 0.15 mg/cm^2 and d of 10 and 20 mm, respectively. The results, with the standard deviation of 2.1% to 7.4%, are shown in Figure 9.

Figure 9. Relationship between $U_{50\%}$ and SDD of composite insulators covered with ice.



As shown in Figure 9, $U_{50\%}$ of the three types of composite insulators also decreases with the SDD , and the relationship between $U_{50\%}$ and SDD follows the same trend as for porcelain and glass insulator strings, *i.e.*, $U_{50\%}$ and SDD are in a negative exponential power function relationship. Results of Figure 9 are fitted according to Equation (4) to obtain the values of related parameters A_s , b , and correlation coefficient R^2 (Table 6).

Table 6. Fitting values of A_s , b , and R^2 according to the test results in Figure 9 with Equation (4).

Type	Ice thickness d (mm)	Fitting values	H (m)/ P (kPa)			
			232/98.6	1000/89.8	2000/79.5	3000/70.1
A	10	A_s	93.8	89.7	85.7	79.2
		b	0.201	0.192	0.191	0.191
		R^2	0.995	0.998	0.996	0.992
	20	A_s	82.1	78.4	75.3	70.5
		b	0.188	0.186	0.180	0.177
		R^2	0.987	0.991	0.987	0.996
B	10	A_s	99.8	92.6	89.5	83.8
		b	0.195	0.196	0.191	0.184
		R^2	0.997	0.996	0.996	0.993
	20	A_s	86.5	82.2	78.2	73.5
		b	0.185	0.184	0.181	0.178
		R^2	0.994	0.997	0.993	0.992s
C	10	A_s	149.3	140.6	131.8	122.8
		b	0.191	0.188	0.184	0.181
		R^2	0.988	0.982	0.985	0.983
	20	A_s	131.1	124.6	115.8	109.4
		b	0.187	0.184	0.182	0.176
		R^2	0.996	0.994	0.992	0.996

The following conclusions can be obtained from Figure 9 and Table 6:

(i) Characteristic exponent b , an indicator of the effects of SDD on $U_{50\%}$ for DC composite insulators, is 0.176 to 0.201 and is related to composite insulator shed profile, altitude or atmospheric pressure, and ice thickness, among other factors.

(ii) b is related to altitude or atmospheric pressure. It decreases with the increase of altitude or the decrease of atmospheric pressure, just as porcelain and glass insulator strings do. For example, for Type C UHV DC composite insulator, when d is 10 mm and P is 98.7, 89.8, 79.5, and 70.1 kPa, b is 0.191, 0.188, 0.184, and 0.181, respectively. That is, the higher the altitude or the lower the atmospheric pressure, the lesser the effects of pollution severity before icing on the DC flashover voltage of ice-covered insulator strings.

(iii) b is related to the ice thickness d . The general tend is that with the growing ice thickness, b becomes smaller, that is, with the increase of ice thickness, the flashover voltage of insulator strings is less affected by SDD . For example, for Type A DC composite insulators, when P is 98.7 kPa, with $d = 10$ mm, b is 0.201; with $d = 20$ mm, b is 0.188.

(iv) b is related to the shed profile, which exerts greater effect than the porcelain and glass insulator structure. For example, with $P = 98.9$ kPa and $d = 10$ mm, b is 0.201 for Type A, 0.195 for Type B, and 0.191 for Type C composite insulator.

3.1.3. The Effects of Atmospheric Pressure on $U_{50\%}$

Most research worldwide shows that with the increase of altitude and the decrease of atmospheric pressure, DC icing flashover $U_{50\%}$ of ice-covered insulators decrease, and DC icing flashover $U_{50\%}$ and P are in a nonlinear relationship as shown below [31]:

$$U_{50\%} = U_0 \left(\frac{P}{P_0}\right)^n \tag{5}$$

where $U_{50\%}$ and U_0 , respectively, represent 50% DC icing flashover voltage of ice-covered insulators at the atmospheric pressure of P and at the standard atmospheric pressure ($P_0 = 101.3$ kPa), and n is the characteristic exponent showing the effects of atmospheric pressure.

Fitting the results in Figures 8 and 9 according to Equation (5) to get U_0 , n , and correlation coefficient R^2 (Tables 7 and 8, respectively) with the fitting curve shown in Figures 10 and 11, respectively.

Figure 10. Relationship between $U_{50\%}$ and P/P_0 of insulator strings covered with ice.

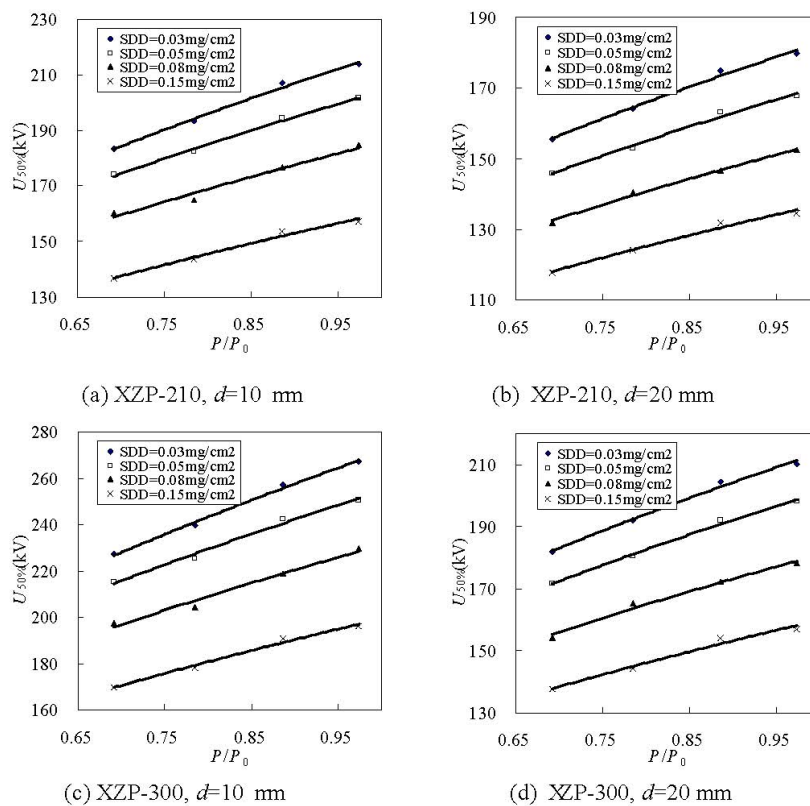


Figure 10. Cont.

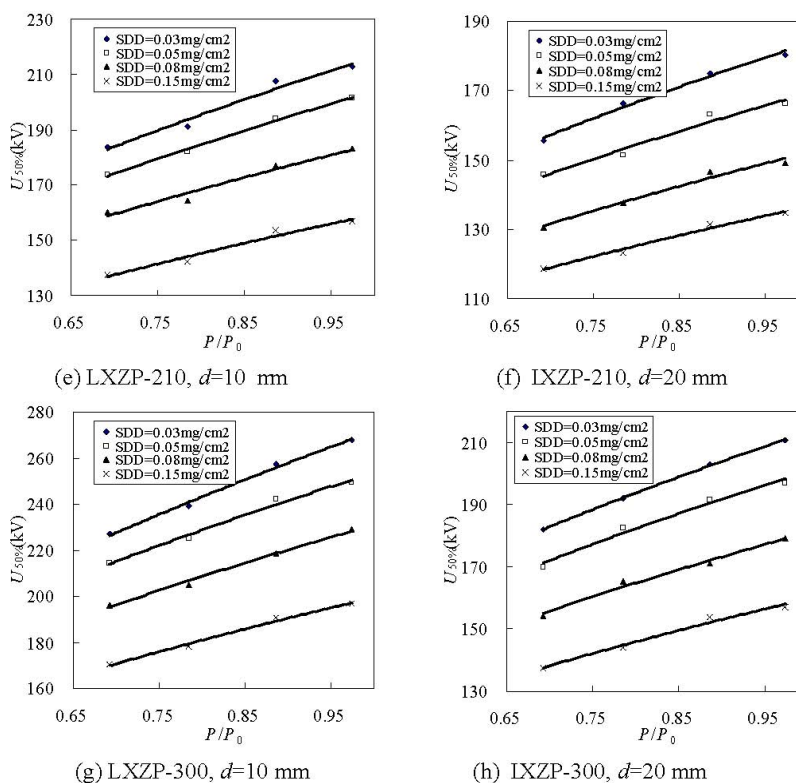


Figure 11. Relationship between $U_{50\%}$ and P/P_0 of composite insulators covered with ice.

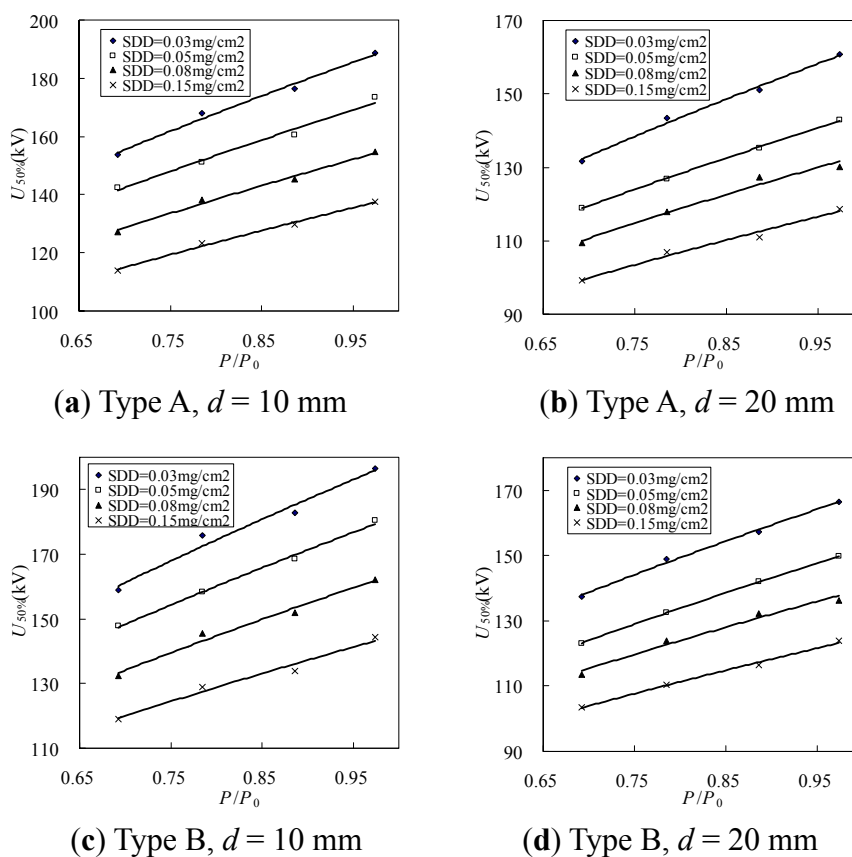
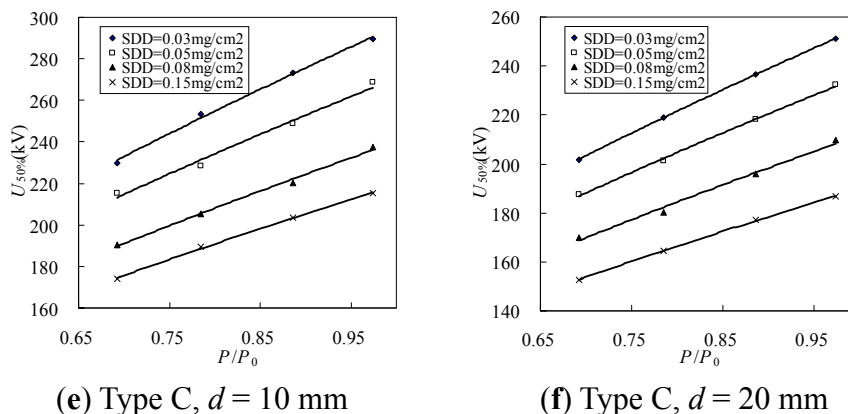


Figure 11. Cont.



The following can be concluded from Figures 10 and 11, Tables 7 and 8:

(i) The characteristic exponent n , which expresses the effects of atmospheric pressure on $U_{50\%}$, is 0.387 to 0.668 for all porcelain, glass insulator strings, and DC composite insulators. It is related to SDD, insulator type, ice thickness, etc.

(ii) n is related to the insulator type. For example, with $SDD = 0.03 \text{ mg/cm}^2$ and $d = 10 \text{ mm}$, n is 0.462 for XZP-210 DC porcelain insulator, 0.485 for XZP-300 DC porcelain insulator, 0.456 for LXZP-210 DC glass insulator, 0.496 for LXZP-300 DC glass insulator, 0.578 for Type A DC composite insulator, 0.590 for Type B composite insulator, and 0.668 for Type C composite insulator.

Table 7. Fitting values of U_0 , n , and R^2 according to the test results in Figure 8 with Equation (5).

Type	Ice thickness d (mm)	Fitting values	SDD (mg/cm ²)			
			0.03	0.05	0.08	0.15
XZP-210	10	U_0	217.2	203.9	185.7	160.0
		n	0.462	0.440	0.427	0.425
		R^2	0.992	0.995	0.973	0.984
	20	U_0	182.7	170.4	154.3	136.9
		n	0.435	0.424	0.416	0.404
		R^2	0.991	0.991	0.993	0.986
XZP-300	10	U_0	271.0	254.1	231.0	199.2
		n	0.486	0.460	0.450	0.427
		R^2	0.995	0.987	0.979	0.990
	20	U_0	213.8	200.9	180.9	159.9
		n	0.434	0.429	0.416	0.403
		R^2	0.993	0.994	0.986	0.980
LXZP-210	10	U_0	216.4	203.9	184.7	159.3
		n	0.456	0.445	0.413	0.413
		R^2	0.972	0.994	0.963	0.971
	20	U_0	183.5	169.2	152.1	136.5
		n	0.435	0.413	0.407	0.387
		R^2	0.989	0.970	0.978	0.985
LXZP-300	10	U_0	271.8	253.7	231.1	199.5
		n	0.496	0.462	0.458	0.436
		R^2	0.994	0.987	0.993	0.990
	20	U_0	213.4	200.7	181.1	159.7
		n	0.432	0.431	0.421	0.405
		R^2	0.997	0.982	0.986	0.979

Table 8. Fitting values of U_0 , n , and R^2 according to the test results in Figure 9 with Equation (5).

Type	Ice thickness d (mm)	Fitting values	SDD (mg/cm ²)			
			0.03	0.05	0.08	0.15
Type A	10	U_0	191.0	173.9	156.5	139.3
		n	0.578	0.561	0.551	0.537
		R^2	0.989	0.981	0.992	0.992
	20	U_0	162.9	144.5	133.4	119.6
		n	0.565	0.533	0.525	0.504
		R^2	0.993	0.999	0.976	0.982
Type B	10	U_0	199.0	182.1	164.4	145.2
		n	0.590	0.575	0.569	0.536
		R^2	0.975	0.995	0.982	0.977
	20	U_0	168.9	152.1	139.7	124.7
		n	0.551	0.572	0.538	0.515
		R^2	0.995	0.997	0.981	0.993
Type C	10	U_0	295.7	270.7	240.1	219.2
		n	0.668	0.649	0.641	0.620
		R^2	0.987	0.982	0.995	0.998
	20	U_0	255.5	235.6	211.7	189.9
		n	0.638	0.629	0.617	0.590
		R^2	0.996	0.995	0.990	0.991

Thus, under the condition of $SDD = 0.03$ mg/cm² and $d = 10$ mm, the effects of atmospheric pressure on DC flashover voltage is the biggest for LXZP-210 insulators and the smallest for Type C composite insulators.

(iii) The characteristic exponent n , which indicates the effects of atmospheric pressure of DC flashover voltage of insulators, is related to SDD . The general trend is that with the growing SDD , n gradually decreases; that is, the more serious the pollution, the less the effects of atmospheric pressure on $U_{50\%}$. For instance, for XZP-210 DC porcelain insulator strings, when SDD is 0.03, 0.05, 0.08, and 0.15 mg/cm², respectively; and d is 10 mm, n is 0.462, 0.440, 0.427, and 0.425 respectively. For Type C UHV DC composite insulators, when SDD is 0.03, 0.05, 0.08, and 0.15 mg/cm² and d is 10 mm, n is 0.668, 0.649, 0.641, and 0.620, respectively.

(iv) Ice thickness d has an effect on characteristic exponent n . The thicker the ice thickness of the monitoring cylinder, the smaller the value of n and the lesser the atmospheric pressure effects on flashover voltage. For instance, for XZP-210 DC porcelain insulator string, when SDD is 0.03 mg/cm² and d is 10 and 20 mm, respectively, n is 0.462 and 0.435. For Type C UHV DC composite insulators, when SDD is 0.03 mg/cm² and d is 10 and 20 mm, respectively, n is 0.668 and 0.638.

3.2. Correction of DC Flashover Voltage for Insulators (string) under Combined Conditions of High Altitude, Pollution, and Icing

DC $U_{50\%}$ of ice-covered insulator strings is subject to the influence of ice thickness, pollution severity on insulator surface, altitude, and insulator structure, among other factors. This study conducted many experiments to obtain $U_{50\%}$ of DC porcelain insulators XZP-210 and XZP-300 DC glass insulators; LXZP-210 and LXZP-300 DC glass insulators; and Types A, B, and C DC composite insulators under different conditions of ice thickness, pollution severity, and altitudes. It also analyzes

the effects of ice thickness, pollution degree, and atmospheric pressure on $U_{50\%}$, and obtains the related characteristic exponents. From the analysis presented above, the influence of ice thickness, pollution degree, or atmospheric pressure on $U_{50\%}$ is known to be affected by other factors obviously or otherwise. UHV transmission lines usually need to cross regions of high altitude, pollution, and icing or regions of such combined conditions. To reduce designers' workload in designing external insulation for transmission lines, an easy and viable correction method for flashover voltage must be set up which can take into account the factors of high altitude, pollution, and icing.

Based on the analysis above, 50% icing flashover voltage $U_{50\%}$ is in negative exponential power function relation with ice thickness d and SDD , and in power function relation with P/P_0 . Thus, the following function is assumed to exist among $U_{50\%}$, d , SDD , and P/P_0 :

$$U_{50\%} = q \times d^{-c} \times SDD^{-b} \times \left(\frac{P}{P_0}\right)^n \quad (6)$$

where q is constant; b , c , and n are the characteristic exponents showing the effects of ice thickness, pollution severity before icing, and atmospheric pressure, respectively.

Based on the experimental results of all the insulator strings above, we convert all the experimental results of $U_{50\%}$ of insulator strings into $U_{50\%}$ per unit spacing of insulator string (dry arcing distance of composite insulator) according to Equation (7). Afterward, we conduct a statistical analysis using MATLAB software and do nonlinear fitting to the data according to Equation (6) through the Levenberg–Marquardt and Universal Global Optimization Methods. The computing formula of $U_{50\%}$ for XZP-210 and XZP-300 DC porcelain insulators, LXZP-210 and LXZP-300 DC glass insulators, Types A, B, and C DC composite insulators can be obtained in terms of per unit spacing (dry arc distance), with the constant q and exponents c , b , and n shown in Table 9:

$$E_{50\%} = \frac{U_{50\%}}{h} \quad (7)$$

In Equation (7), h is the unit spacing for porcelain and glass insulators or dry arc distance for composite insulators.

Table 9. Fitting values of q , c , b , n , and R^2 according to the test results of typical insulators with Equation (6).

Type	Fitting values				Correlation coefficient
	q	c	b	n	R^2
XZP-210	70.3	0.209	0.192	0.429	0.979
XZP-300	104.4	0.288	0.193	0.433	0.978
LXZP-210	70.2	0.210	0.193	0.425	0.978
LXZP-300	104.9	0.289	0.192	0.435	0.983
Type A composite insulator	74.8	0.221	0.187	0.435	0.993
Type B composite insulator	75.0	0.219	0.184	0.559	0.992
Type C composite insulator	66.7	0.195	0.186	0.638	0.994

The maximum error between results calculated by Equations (6) and (7) based on the fitting values in Table 9 and the results gained by experiments is 6.9%. Using Equations (6) to (7) and the

parameters in Table 9 it is viable to obtain related data for the design of the outer insulation of transmission lines. However, due to the limited amount of experimental results of the present study, numerous experiments are suggested to verify and improve the dependability and applicable range of parameters in Table 9.

4. Conclusions

The icing flashover performance tests of typical DC porcelain (*i.e.*, XZP-210 and XZP-300), glass (*i.e.*, LXZP-210 and LXZP-300), and three types of shed-profile composite insulators are systematically carried out under various combined conditions (different ice thickness, SDD, and pressure) in a multifunction artificial climate chamber. Results show the following:

(i) $U_{50\%}$ decreases with increasing ice thickness of the monitoring cylinder, following a negative exponential power function and its characteristic exponent, which is related to insulator type, contamination condition, atmospheric pressure, etc., with a varying range of 0.182 to 0.288;

(ii) $U_{50\%}$ decreases with increasing SDD before icing, following a negative exponential power function. The characteristic exponent of SDD is relative to insulator type, atmospheric pressure, ice thickness, etc. (that is, the lower the atmospheric pressure and the thicker the ice, the smaller the exponent) with a value ranging from 0.173 to 0.210;

(iii) $U_{50\%}$ and the ratio of air pressure (P/P_0) are in a power function relationship, and the characteristic exponent is related to insulator type, contamination condition, and ice thickness (that is, the more serious the contamination condition and the thicker the ice, the smaller the exponent n) with a value range of 0.387 to 0.668.

The DC icing flashover voltage correction method of typical porcelain, glass, and composite insulator in the coexisting conditions of high altitude, contamination, and icing is put forward. The method is expressed as $U_{50\%} = q \times d^c \times SDD^{-b} \times (P/P_0)^n$, where the coefficient q and exponents c , b , and n of seven typical insulators under various icing thickness, SDD, string length, and atmospheric pressure are gained.

Acknowledgments

This work was supported by Key Project of Chinese National Programs for Fundamental Research and Development (973 program) (2009CB724502); project supported by the Funds for Innovative Research Groups of China (51021005); project supported the National Science Foundation of China (Project No. 51107152); project Supported by the Fundamental Research Funds for the Central Universities (No. CDJRC10150005).

References

1. Meier, A.; Niggli, W.M. The Influence of Snow and Ice Deposits on Supertension Transmission Line Insulator Strings with Special Reference to High Altitude Operations. *IEEE Conf. Proc.* **1968**, *44*, 386–395.

2. Cherney, E.A. Flashover performance of artificially contaminated and iced long-rod transmission line insulators. *IEEE Trans. Power App. Syst.* **1980**, PAS-999, 46–52.
3. Matsuda, H.; Komuro, H.; Takasu, K. Withstand voltage characteristics of insulator strings covered with snow or ice. *IEEE Trans. Power Deliv.* **1991**, 6, 1243–1250.
4. Farzaneh, M.; Kiernicki, J. Flashover problems caused by ice build-up on insulators. *IEEE Elec. Insul. Mag.* **1995**, 11, 5–17.
5. Influence of ice and snow on the flashover performance of outdoor insulators Part I: Effects of ice. CIGRE Task Force 33.04.09 Report. *Électra* **1999**, 187, 90–111.
6. Kannus, K.; Lahti, K. Electrical behaviour of high voltage insulator strings under rime ice. In *Proceedings of the 9th International Workshop on Atmospheric Icing of Structures*, Chester, UK, 5–8 June 2000; p. 8.
7. Jiang, X.L.; Shu, L.C.; Sima, W.X.; Xie, S.J.; Hu, J.L.; Zhang, Z.J. Chinese transmission lines' icing characteristics and analysis of severe ice accidents. *Int. J. Offshore Polar Eng.* **2004**, 14, 196–201.
8. Fikke, S.M.; Hanssen, J.E.; Rolfseng, L. Long range transported pollution and conductivity on atmospheric ice on insulators. *IEEE Trans. Power Deliv.* **1993**, 8, 1311–1321.
9. Farzaneh, M.; Drapeau, J.F. AC flashover performance of insulators covered with artificial ice. *IEEE Trans. Power Deliv.* **1995**, 10, 1038–1051.
10. Farzaneh, M.; Kiernicki, J. Flashover performance of IEEE standard insulators under ice conditions. *IEEE Trans. Power Deliv.* **1997**, 12, 1602–1613.
11. Farzaneh, M.; Baker, T.; Bernstorff, A.; Brown, K.; Chisholm, W.A.; de Turreil, C.; Drapeau, J.F.; Fikke, S.; George, J.M.; Gnanndt, E.; *et al.* Insulator icing test methods and procedures: A position paper prepared by the IEEE task force on insulator icing test methods. *IEEE Trans. Power Deliv.* **2003**, 18, 1503–1515.
12. Li, Q.F.; Fan, Z.; Wu, Q.; Gao, J.; Su, Z.Y.; Zhou, W.J. Investigation of ice-covered transmission lines and analysis on transmission line failures caused by ice-coating in China. *Power Syst. Technol.* **2008**, 9, 33–36.
13. Hu, Y. Analysis and countermeasures discussion for large area icing accident on power grid. *High Volt. Eng.* **2008**, 2, 215–219.
14. Jiang, X.L. Accident analysis of Guizhou power grid ice hazard and its countermeasures. *Electr. Power Constr.* **2008**, 4, 1–4.
15. Lu, J.Z.; Jiang, Z.L.; Lei, H.C.; Zhang, H.X.; Peng, J.W.; Li, B.; Fang, Z. Analysis of Hunan power grid ice disaster accident in 2008. *Autom. Electr. Power Syst.* **2008**, 11, 16–19.
16. Fofana, I.; Farzaneh, M. Process of discharge initiation and arc development on an ice-covered insulator. In *Proceedings of Transmission and Distribution Conference and Exhibition, 2005/2006 IEEE PES*, Dallas, TX, USA, 21–24 May 2006; pp. 115–120.
17. Farzaneh, M. Ice accretion on high voltage conductors and insulators and related phenomena. *Philos. Trans. R. Soc. Lond. A* **2000**, 1776, 2971–3005.
18. Zhang, J.; Farzaneh, M. Propagation of AC and DC arcs on ice surfaces. *IEEE Trans. Dielectr. Electr. Insul.* **2000**, 7, 269–276.
19. Farzaneh, M.; Zhang, J. A multi-arc model for predicting ac critical flashover voltage of ice-covered insulators. *IEEE Trans. Dielectr. Electr. Insul.* **2007**, 14, 1401–1409.

20. Farzaneh, M. *Atmospheric Icing of Power Networks*; Springer: Berlin, Germany, 2008; pp. 269–323.
21. Jiang, X.L.; Sun, C.X. Study on AC flashover performance and process of ice-covered 10 kV composite insulator. *Proc. CSEE* **2002**, *22*, 58–61.
22. Sun, C.X.; Jiang, X.L.; Shu, L.C.; Sima, W.X.; Gu, L.G. AC/DC flashover performance and its voltage correction of UHV insulators in high altitude and icing and pollution environments. *Proc. CSEE* **2002**, *11*, 115–120.
23. Tian, Y.C.; Jiang, X.L.; Shu, L.C. AC flashover performance and voltage correction of iced 10 kV composite insulator in high altitude area. *High Volt. Eng.* **2002**, *6*, 13–15.
24. Wu, L.H.; Jiang, X.L.; Xiong, Q.X.; Sima, W.X.; Sun, C.X. DC flashover performance and voltage correction of iced XZP-160 insulator at low atmospheric pressure. *High Volt. Eng.* **2002**, *10*, 5–7.
25. Yi, H.; Wang, L.Q. Measures of preventing ice flashover for transmission line insulator string and analysis of mechanism. *High Volt. Eng.* **2003**, *29*, 57–58.
26. Sima, W.X.; Jiang, X.L.; Wu, L.H.; Shu, L.C.; Sun, C.X. DC electrical performance of icing and polluted 10 kV composite insulator at low atmospheric pressures. *Proc. CSEE* **2004**, *7*, 122–126.
27. Jiang, X.L.; Xie, S.J.; Shu, L.C. Ice flashover performance and comparison on three types of DC insulators at low atmosphere pressure. *Proc. CSEE* **2004**, *9*, 158–162.
28. Yuan, J.H.; Jiang, X.L.; Zhang, Z.J.; Hu, J.L.; Sun, C.X. Study on dc flashover performance of three types of iced post insulators at lower atmospheric pressure. *Proc. CSEE* **2005**, *15*, 12–15.
29. Jiang, X.L.; Wu, L.H.; Sima, W.X.; Shu, L.C.; Sun, C.X. Study on flashover mechanism of XZP/XZWP4-160 DC insulator under icing and low atmospheric pressure conditions. *Proc. CSEE* **2004**, *6*, 111–115.
30. Jiang, X.L.; Wang, S.H.; Zhang, Z.J.; Xie, S.J.; Wang, Y. Study on AC flashover performance and discharge process of polluted and iced IEC standard suspension insulator string. *IEEE Trans. Power Deliv.* **2007**, *22*, 472–480.
31. Hu, J.L.; Sun, C.X.; Jiang, X.L.; Shu, L.C. Flashover performance of pre-contaminated and ice-covered composite insulators to be used in 1000 kV UHV AC transmission lines. *IEEE Trans. Dielectr. Electr. Insul.* **2007**, *14*, 1347–1356.
32. Li, P.; Fan, J.B.; Li, W.F.; Su, Z.Y.; Zhou, J. Flashover performance of hvdc iced insulator strings. *IEEE Trans. Dielectr. Electr. Insul.* **2007**, *6*, 1334–1338.
33. Farzaneh, M.; Baker, A.C.; Allen Bernstorff, R.; Burnhan, J.T.; Cherney, E.A.; Chisholm, W.A.; Gorur, R.S.; Grisham, T.; Gutman, I.; Rolfseng, L.; *et al.* Selection of line insulators with respect to ice and snow, part i: context and stresses. *IEEE Trans. Power Deliv.* **2007**, *4*, 2298–2296.
34. International Electrotechnical Commission (IEC). *Artificial Pollution Tests on High-Voltage Insulators to Be Used on A.C. Systems*; Technical Report IEC 60507; IEC: Geneva, Switzerland, 1991.
35. *IEEE Guide for Test Methods and Procedures to Evaluate the Electrical Performance of Insulators in Freezing Conditions*; IEEE Standard 1783–2009; The Institute of Electrical and Electronics Engineers, Inc.: New York, NY, USA, 2009.